

# The Effects of Respiratory Muscle Training on Resting-State Brain Activity and Thoracic Mobility in Healthy Subjects: A Randomized Controlled Trial

Naciye Vardar-Yagli, PT, PhD,<sup>1\*</sup>  Melda Saglam, PT, PhD,<sup>1</sup> Hacer Dasgin, PhD,<sup>2</sup> and Kader Karli-Oguz, MD<sup>2,3</sup>

**Background:** Although inspiratory muscle training (IMT) is an effective intervention for improving breath perception, brain mechanisms have not been studied yet.

**Purpose:** To examine the effects of IMT on insula and default mode network (DMN) using resting-state functional MRI (RS-fMRI).

**Study Type:** Prospective.

**Population:** A total of 26 healthy participants were randomly assigned to two groups as IMT group ( $n = 14$ ) and sham IMT groups ( $n = 12$ ).

**Field Strength/Sequence:** A 3-T, three-dimensional T2\* gradient-echo echo planar imaging sequence for RS-fMRI was obtained.

**Assessment:** The intervention group received IMT at 60% and sham group received at 15% of maximal inspiratory pressure (MIP) for 8 weeks. Pulmonary and respiratory muscle function, and breathing patterns were measured. Groups underwent RS-fMRI before and after the treatment.

**Statistical Tests:** Statistical tests were two-tailed  $P < 0.05$  was considered statistically significant. Student's  $t$  test was used to compare the groups. One-sample  $t$ -test for each group was used to reveal pattern of functional connectivity. A statistical threshold of  $P < 0.001$  uncorrected value was set at voxel level. We used False discovery rate (FDR)-corrected  $P < 0.05$  cluster level.

**Results:** The IMT group showed more prominent alterations in insula and DMN connectivity than sham group. The MIP was significantly different after IMT. Respiratory rate ( $P = 0.344$ ), inspiratory time ( $P = 0.222$ ), expiratory time ( $P = 1.000$ ), and inspiratory time/total breath time ( $P = 0.572$ ) of respiratory patterns showed no significant change after IMT. All DMN components showed decreased, while insula showed increased activation significantly.

**Data Conclusion:** Differences in brain activity and connectivity may reflect improved ventilatory perception with IMT with a possible role in regulating breathing pattern by processing interoceptive signals.

**Evidence Level:** 2

**Technical Efficacy:** Stage 4

J. MAGN. RESON. IMAGING 2023;57:403–417.

Understanding of the sensory perception of breathing patterns in healthy individuals and chronic diseases has increased owing to advances in neuroimaging.<sup>1</sup> The link between learned associations and respiration has been well proven in several experimental studies that used conditioning to show how associative learning affects respiratory perception

and brain processing.<sup>2,3</sup> Information and predictions about the body status and emotions, such as breath perception, are generated in the anterior insula, anterior cingulate cortex (ACC), orbitofrontal cortex, and ventromedial prefrontal cortex. The periaqueductal gray matter feed sensory information into these networks.<sup>2</sup> Blood oxygen level-dependent (BOLD)

View this article online at [wileyonlinelibrary.com](http://wileyonlinelibrary.com). DOI: 10.1002/jmri.28322

Received Apr 13, 2022, Accepted for publication Jun 14, 2022.

\*Address reprint requests to: N.V.-Y., Faculty of Health Sciences, Department of Cardiorespiratory Physiotherapy and Rehabilitation, Hacettepe University, Samanpazari, Altindag, Ankara, Turkey. E-mail: [naciyevardar@yahoo.com](mailto:naciyevardar@yahoo.com)

From the <sup>1</sup>Hacettepe University, Faculty of Physical Therapy and Rehabilitation, Department of Cardiorespiratory Physiotherapy and Rehabilitation, Ankara, Turkey; <sup>2</sup>National Magnetic Resonance Research Center (UMRAM) Bilkent University, Ankara, Turkey; and <sup>3</sup>Hacettepe University, Faculty of Medicine, Department of Radiology, Ankara, Turkey

contrast is used in functional MRI (fMRI) as an indirect indicator of brain neuronal activity.<sup>4</sup> The default mode network (DMN) is one of the well-studied resting-state networks. During a wide range of cognitive or goal-directed processes, DMN is a set of brain areas that are often found deactivated.<sup>5</sup>

Inspiratory muscle training (IMT) is one of the most effective interventions for improving breath perception in healthy people. The IMT has shown benefits including maintaining pressure generation, promoting inspiratory muscle hypertrophy and increasing the proportion of type I fibers, attenuating the respiratory muscle metaboreflex, reducing the rating of dyspnea or perceived exertion, improving respiratory muscle economy, and reducing the work of breathing.<sup>6–8</sup> It improves respiratory muscle function, lung function, and exercise capacity.<sup>9</sup> The efficacy of IMT has been investigated extensively both in healthy people and patients with chronic respiratory illnesses, although the results are still controversial.<sup>10,11</sup> Hart et al conducted a 6-week prospective randomized controlled trial in which 12 healthy volunteers were randomly assigned to either IMT or sham IMT training. The training group's maximal inspiratory pressure (MIP) increased, but there was no change in exercise performance.<sup>11</sup> In chronic diseases such as chronic obstructive pulmonary disease (COPD), however, the perception of breathlessness has been shown to decrease after IMT intervention.<sup>12</sup> Exercise training reduced dyspnea intensity and anxiety in COPD patients, with associated alterations in the brain's processing of breathlessness-related words, according to a study.<sup>2</sup> In healthy individuals or people with chronic respiratory diseases, the brain mechanisms underpinning this issue have yet to be studied.<sup>13</sup>

After IMT, the measurement of breathing pattern provides vital information on respiratory mechanics and breathing control.<sup>14</sup> Structured light plethysmography (SLP) is a unique light-based technology that allows for extensive analysis of breathing patterns.<sup>14</sup> The SLP is a noncontact, noninvasive procedure that does not involve the use of a mouthpiece, nasal clip, or any other equipment. SLP technology allows clinicians to acquire breathing pattern measurements that are more ecologically relevant than those obtained by spirometry.<sup>15</sup> Current pulmonary function testing methods are unable to distinguish the contribution rates of different areas of the lungs during breathing. Through movement of the chest wall, the SLP provides real-time regional respiratory function.<sup>15</sup> A clinically meaningful indicator of the relative contribution of the right and left sides of the thoracoabdominal wall in these individuals could help guide the effectiveness of interventions as IMT.

Hence, the present study aimed to determine the occurrence of alterations in brain activity after high-intensity IMT in DMN and insula networks of resting-state fMRI (RS-fMRI) compared with sham treatment and if so, the interaction between these network activation changes and lung function, respiratory muscle strength and endurance.

## Materials and Methods

### Participants

The research was approved by the local ethics committee and carried out in accordance with the Declaration of Helsinki. The participants signed a written informed consent. The inclusion criteria were ages of 18–65 years, right-handed, and healthy. Only right-handed participants were included in this study to keep uniformity within the groups and use the standard knowledge existing in the literature where the majority of studies were performed on right-handed subjects. The exclusion criteria were as follows: chronic or recurrent bronchial/lung disease, smokers, pregnancy, respiratory tract infection in the last 6 weeks, restrictive disease, neurological disease, chronic pain conditions, mental health problems, use of drugs that may affect the respiratory system or introspective focus in the last 7 days, alcohol use in the last 2 days, drug/substance use with a central nervous system stimulants or depressive effect, physical conditions that may have high basal breathing capacity and thus brain activity, claustrophobia, or contraindication for MRI.

### Study Design

This study was a randomized controlled trial with a prospective design. It was conducted at Hacettepe University, Faculty of Physical Therapy and Rehabilitation, Department of Cardiorespiratory Physiotherapy and Rehabilitation Unit and National Magnetic Resonance Research Center between September 2019 and January 2021. IMT was given to the intervention group, whereas sham IMT was defined as the control group. An inspiratory threshold-loading device was used to train the individuals (Powerbreathe®, Southam, UK). The IMT group was given to the intervention group at 60% of MIP. The sham IMT group was given to the control group at a predetermined workload of 15% of MIP. For 8 weeks, both groups trained for 30 minutes a day, 5 days a week.

The required sample size for each group comprised a minimum of 12 subjects based on type I error of 0.05 and type II error of 0.20 with the power 80% by a power analysis program (G\*Power, version 3.1., Universität Düsseldorf, Düsseldorf, Germany). A total of 39 healthy individuals ( $27.15 \pm 4.02$  years, 20 females, 19 males) were enrolled according to the inclusion and exclusion criteria. All individuals were evaluated clinically prior to randomization. Based on a program ([www.randomizer.org](http://www.randomizer.org)) to generate random numbers using simple random sampling, subjects were randomly assigned to either the intervention ( $n = 21$ ) or sham group ( $n = 18$ ). Three subjects from the sham group and two subjects from the intervention group withdrew, and three subjects from each group did not continue to treatment, and fMRI of three subjects from IMT group could not be analyzed because of unacceptable head motion with maximum translation error exceeding 2 mm. Therefore, 14 subjects in the IMT group and 12 subjects in the sham group were included in the analyses (Fig. 1). Neither the participants nor the clinicians were aware of the groups to which patients had been allocated. Neither the participants nor the clinicians were aware of the groups to which patients had been allocated. The research was reported in line with the Consolidated Standards of Reporting Trials (CONSORT) guidelines.

Demographic data including the participants' age, gender, weight, height, and body mass index were recorded. Pulmonary function, respiratory muscle strength, respiratory muscle endurance,

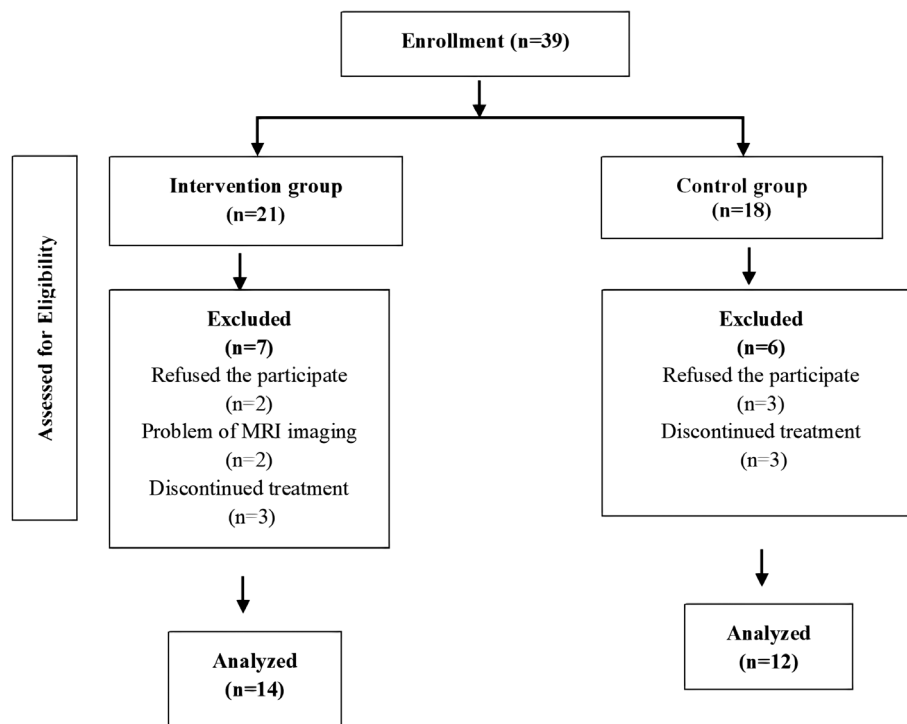


**FIGURE 1: Flowchart of the participants.**

chest and abdominal wall movements, and fMRI were all assessed before and after the training.

### Pulmonary Function Testing

The pulmonary function testing was carried out using a portable spirometer (MIR II Spirolab™, Medical International Research, Italy) in accordance with the American Thoracic Society and the European Respiratory Society's guidelines. The percentages of predicted values for forced vital capacity (FVC), forced expiratory volume in 1 second (FEV<sub>1</sub>), FEV<sub>1</sub>/FVC, and peak expiratory flow (PEF) were measured.<sup>16</sup>

### Respiratory Muscle Strength and Endurance Testing

A mouth pressure device (MicroRPM, CareFusion UK 232 Ltd., Basingstoke, UK) was used to measure the MIP and maximal expiratory pressure (MEP). The MIP was measured near residual volume

following a maximal expiration while the MEP was assessed near total lung capacity after a maximal inspiration. The tests were repeated until no further improvements were obtained and the difference between the two best values was less than 10%.<sup>17</sup>

A threshold loading inspiratory muscle trainer (Powerbreathe®) was used to perform the respiratory muscle endurance testing. The inspiratory threshold load was set to 60% of MIP in this study. During loaded breathing, they were told to inhale deeply and maintain a constant respiratory rate. During loaded breathing, individuals were told to inhale deeply and maintain a constant respiratory rate. When the subject was unable to open the limit valve for three consecutive breaths, or when the subject was unable to continue the test and had to evacuate the mouthpiece, the test was over. The total time was recorded and the maximum duration of the test was limited to 10 minutes.<sup>17</sup>

The dynamic inspiratory pressure (strength index) was measured using a handheld loading device, named Powerbreathe K5 inspiratory muscle trainer (HaB Ltd, Southam, UK). All patients

**TABLE 1. Demographic Characteristics of Healthy Subjects**

Characteristics	IMT Group (n = 14) Mean (SD)	Sham Group (n = 12) Mean (SD)	P value
Age, year	25.6 (1.9)	28.8 (5.6)	0.118
Female; male (n)	7/7	8/4	0.453
Weight, kg	67 (14.1)	65.4 (11.1)	0.860
Height, cm	172.1 (9.5)	166.3 (8.2)	0.176
Body mass index, kg/m <sup>2</sup>	22.4 (2.7)	23.7 (3.6)	0.274

IMT = inspiratory muscle training.

**TABLE 2. Effects of IMT on Lung Function and Respiratory Muscle Function**

Variables	IMT Group (n = 14)			Sham Group (n = 12)			Between Groups P value
	Baseline	After	Group Differences P value	Baseline	After	Group Differences P value	
	Mean (SD)	Mean (SD)		Mean (SD)	Mean (SD)		
FEV <sub>1</sub> (%)	102.4 (13.4)	99.5 (11.2)	0.145	97.5 (11.2)	97.8 (11.9)	0.906	0.648
FVC (%)	107.7 (14.8)	105.6 (13.6)	0.208	102.4 (10.9)	101.8 (9.9)	0.932	0.483
FEV <sub>1</sub> /FVC	84.8 (3.0)	80.8 (4.7)	0.046 <sup>a</sup>	82.8 (3.5)	81.3 (5.4)	0.593	0.832
PEF (L/minute)	109.1 (17.2)	106 (14.4)	0.675	105 (8.7)	102.9 (21.2)	0.312	0.101
MIP (cmH <sub>2</sub> O)	114.4 (30.6)	132.4 (31.7)	0.023 <sup>a</sup>	115.9 (29.5)	108 (24.3)	0.674	0.030 <sup>b</sup>
MEP (cmH <sub>2</sub> O)	135.6 (39.1)	142.6 (31.0)	0.136	136.6 (41.5)	118.3 (29.5)	0.091	0.110
Strength-index	113.3 (22.6)	130.7 (28.2)	0.003 <sup>a</sup>	101.6 (20.8)	102.1 (17.3)	0.011 <sup>a</sup>	0.012 <sup>b</sup>
PIF	6.3 (1.1)	7.1 (1.4)	0.005 <sup>a</sup>	5.7 (1.1)	5.8 (0.9)	0.021 <sup>a</sup>	0.036 <sup>b</sup>
Endurance time (sec)	373.3 (225.1)	398.4 (207.1)	0.594	424 (262.9)	336.7 (234.4)	0.465	0.705

FEV<sub>1</sub> = forced expiratory volume in 1 second; FVC = forced vital capacity; PEF = peak expiratory volume; MIP = maximal inspiratory pressure; MEP = maximal expiratory pressure; PIF = peak inspiratory flow.  
<sup>a</sup>Significant difference before and after the treatment in each group.  
<sup>b</sup>Significant difference between the groups.

TABLE 3. Effects of IMT on SLP Parameters Between the Groups

Variables	IMT Group ( <i>n</i> = 14)			Sham Group ( <i>n</i> = 12)			Between Groups <i>P</i> value
	Baseline	After	Group Differences	Baseline	After	Group Differences	
	Mean (SD)	Mean (SD)	<i>P</i> value	Mean (SD)	Mean (SD)	<i>P</i> value	
Respiratory rate (breaths/minute)	16.9 (4.0)	17.5 (3.4)	0.937	19.1 (4.1)	18.6 (2.8)	0.722	0.344
$T_i$	1.5 (0.3)	1.6 (0.3)	0.638	1.5 (0.2)	1.4 (0.2)	0.965	0.222
$T_E$	2.2 (0.8)	1.9 (0.4)	0.480	1.9 (0.3)	1.9 (0.3)	0.959	1
$T_i/T_E$	0.7 (0.1)	0.8 (0.1)	0.155	0.8 (0.1)	0.8 (0.1)	0.656	0.609
$T_{tot}$	3.7 (1.0)	3.5 (0.7)	0.724	3.3 (0.5)	3.3 (0.5)	1	0.501
$T_i/T_{tot}$	0.4 (0.04)	0.5 (0.04)	0.227	0.4 (0.04)	0.4 (0.04)	0.572	0.572
RCA (%)	52.9 (8.4)	52 (11.7)	0.814	51.3 (8.5)	51.3 (8.5)	0.759	0.851
IE50	1.5 (0.4)	1.3 (0.3)	0.859	1.3 (0.4)	1.3 (0.4)	0.033	1

$T_i$  = inspiratory time;  $T_E$  = expiratory time;  $T_{tot}$  = total breath time; RCA = relative contribution of abdomen to each breath; IE50 = inspiratory to expiratory thoraco–abdominal displacement rate.

performed at least 30 consecutive maximal inspiratory attempts from residual volume to total lung capacity. Based on peak inspiratory flow (PIF), the strength index (S-index) was calculated using the software included with the device (Breathe-Link, Version 1.0, 2012).<sup>18</sup>

### Chest and Abdominal Wall Movements

The SLP device (Thora-3Di, PneumaCare Ltd, Cambridge, UK) was used to quantify chest and abdominal wall movements during 5 minutes of silent tidal breathing.<sup>19</sup> For SLP data acquisition, subjects were requested to change into a close-fitting white t-shirt that followed the contours of their bodies and SLP data were collected on the bare chest. Participants were instructed to sit in a high-backed chair with their necks in a neutral position and their backs as straight as possible. This produced a one-dimensional signal that was viewed on a computer using PneumaView-3D™ software (PneumaCare Ltd, Cambridge, UK) and corresponded to an individual's tidal breathing pattern. Respiratory rate, inspiratory, and expiratory time ( $T_i$  and  $T_E$ ),  $T_i/T_E$ , and total breath time ( $T_{tot}$ ), and  $T_i/T_{tot}$  (duty cycle) were among the measurements acquired from SLP.<sup>19,20</sup> Inspiratory to expiratory thoracoabdominal displacement rate ratio (IE50) was the flow-based parameter.

### fMRI Studies

**PROTOCOL.** After the individuals participating in the study were evaluated with fMRI, they were taken to IMT for 8 weeks. They were reassessed within 2 days after the training was over. MRI was performed at National Magnetic Resonance Research Center (UMRAM, Bilkent University, Turkey) using a 3-T scanner (Siemens Trio, Germany) magnet equipped with a 32-channel phased array head coil. Structural data included a three-dimensional gradient-echo sequence (3D T1-weighted,

magnetization-prepared rapid gradient-recalled echo, TR/TE = 2600/3.02 msec; FOV = 256 × 256; 176 volumes) with an in-plane resolution (voxel size) of 1 × 1 × 1 mm<sup>3</sup>. An axial T2 turbo spin-echo (TR/TE = 3600/100 msec; FOV = 220 mm) imaging was also obtained to rule out any brain lesion and thus to confirm eligibility of the subjects for this study. All the structural data were evaluated by a neuroradiologist with an experience over 20 years (K.K.O.).

Radiological evaluation revealed no abnormality on structural 3DT1W and axial T2W images of the participants. Resting state-fMRI was obtained using a T2\*-weighted gradient echo planar imaging (TR/TE = 2000/35 msec; matrix = 64 × 64, flip angle = 75°; 184 volumes, voxel size = 3 × 3 × 3 mm<sup>3</sup>; acquisition time = 6.12 minutes).

**fMRI PREPROCESSING.** Preprocessing of RS-fMRI images was performed with statistical parametric mapping12 (SPM12) ([www.fil.ion.ucl.ac.uk/spm/software/spm12](http://www.fil.ion.ucl.ac.uk/spm/software/spm12), University College London, London, United Kingdom) implemented in Matlab2020 (<https://www.mathworks.com>) using standard procedure. First four images of the run were discarded followed by realignment, co-registration, segmentation of functional and structural images, and normalization to the Montreal Neurological Institute (MNI) template using a participant-specific transformation generated by fitting the mean functional images to the echo-planar imaging standard toolbox template. These images were interpolated to 3 × 3 × 3 mm<sup>3</sup> voxels. Smoothing using an 8 mm Gaussian kernel was performed to reduce spatial noise and increase the signal-to-noise ratio. Component-based noise correction method was applied for the reduction of noise in images. Temporal frequencies below 0.008 Hz or above 0.09 Hz were removed from the BOLD signal in order to focus on slow-frequency fluctuations while minimizing the influence of physiological, head-motion, and other noise sources.

**TABLE 4. Significant Clusters ( $P < 0.05$  FDR corrected) Within Default Mode Network in the Groups are Shown in Terms of Cluster Size and Strengths of Activation and Deactivations With MNI  $x, y, z$  Coordinates**

Groups	Regions	Cluster	$t$ value	$x$	$y$	$z$
Baseline variables	Positive					
	MPFC	823	11.9	-6	56	-6
	Left LP	2236	18.2	12	-54	26
	Right LP	1884	18.9	46	-64	32
	PCC	1773	18.2	12	-54	26
Sham group	Negative					
	Right insula	638	-9.9	58	12	6
	Left insula	676	-10.6	-48	14	2
	Positive					
	MPFC	610	10.9	-12	48	-06
IMT group	Left LP	850	5.5	-54	-60	18
	Right LP	1751	7.2	52	-60	14
	PCC	1234	8.2	06	-46	08
	Negative					
	Right insula	433	-8.7	40	8	8
Sham vs. baseline	Left insula	400	-8.9	-44	02	02
	Positive					
	MPFC	603	8.9	4	60	-06
	Left LP	1372	7.5	-42	-72	30
	Right LP	1307	8.9	52	-58	20
IMT vs. baseline	PCC	1047	9.4	16	-52	20
	Right insula	-	-	-	-	-
	Left insula	-	-	-	-	-
IMT vs. baseline	Positive					
	Left postcentral gyrus	65	4.15	-38	-30	54
	Right postcentral gyrus	28	3.42	34	-34	54
	Positive					
	Left insula	241	3.44	-42	-2	6
IMT vs. baseline	Right insula	14	3.65	46	2	6
	Left putamen	241	4.46	-30	-4	8
	Right IFG	20	3.75	62	14	26
	Left IFG	31	3.38	-44	14	8
	Left cerebellum	10	3.49	-26	-58	-58
IMT vs. baseline	Negative					
	Left middle temporal gyrus	70	-3.67	-48	-64	26

TABLE 4. Continued

Groups	Regions	Cluster	<i>t</i> value	<i>x</i>	<i>y</i>	<i>z</i>
	Positive					
	Right insula	80	4.41	46	2	6
	Left insula	8	3.52	-44	0	2
IMT vs. sham	Left IFG	51	4.44	-38	26	2
	Right IFG	24	4.37	40	26	-6
	Left cerebellum	18	3.86	-38	-58	-22
	Negative					
	Right cerebellum	35	-4.48	52	-60	-40

Positive: Activated brain regions to the DMN. Negative: Deactivated brain regions to the DMN.  
 MPFC = medial prefrontal cortex; LP = lateral parietal; PCC = posterior cingulate cortex; IFG = inferior frontal gyrus;  
 IMT = inspiratory muscle training.

#### GENERAL LINEAR MODEL AND SEED-BASED CONNECTIVITY ANALYSIS.

Following preprocessing, the data were analyzed using the general linear model, and these results were used for group analysis using the CONN toolbox (SPM-based cross-platform software for the computation, display, and analysis of functional connectivity).<sup>21</sup> Seed-based connectivity (SBC), which reveals the connectivity patterns with a pre-defined seed, was applied to the data in group analysis for RS networks. SBC maps were computed as the Fisher-transformed bivariate correlation coefficients between a region-of-interest (ROI, which are part of the DMN and Insula) and each individual voxel in the time series. SBC mapping was performed for DMN and bilateral insula network and also for connectivities of these networks with other regions of the brain.

In this study, as defined by the CONN toolbox, the DMN consisted of the posterior cingulate cortex (PCC), medial prefrontal cortex (MPFC), left-right lateral parietal (LP) cortex, while the insula network was composed of right and left insula. The one-sample *t*-test for each group was used to reveal the pattern of functional connectivity including the DMN regions and insula network. Within these networks, brain regions showing correlations with MIP, MEP, S-index, IE50,  $T_i/T_{tot}$  tests also were calculated with regression analysis. Positive and negative correlated regions were marked with red and blue colors, respectively.

#### Statistical Analysis

Data were analyzed using the statistical software package SPSS version 23.0 (IBM Corp., Armonk, NY, USA) and tested using the Kolmogorov-Smirnov calculation for normality. Statistical tests were two-tailed and  $P < 0.05$  was considered statistically significant. Analysis of continuous variables between the groups was completed using the Student's *t* test or Mann-Whitney U test and analysis between IMT and sham groups was performed using the chi-square test (nominal data). Wilcoxon signed rank test was performed for comparison within group before and after the treatment.

A statistical threshold of  $P < 0.001$  uncorrected value was set at voxel level across the whole-brain. For multiple comparison, we used FDR-corrected  $P < 0.05$  cluster-level as recommended by CONN toolbox guide ([https://web.conn-toolbox.org/fmri-methods/cluster-level-inferences#h\\_p\\_CNRvEwPa1Xy2](https://web.conn-toolbox.org/fmri-methods/cluster-level-inferences#h_p_CNRvEwPa1Xy2)). Regions that survived these thresholds were reported as active regions along with their cluster size and *x*, *y*, *z* coordinates according to the MNI atlas. Activation maps and tables were created including *t* values and cluster sizes for both groups. We also compared IMT and sham IMT groups with baseline fMRI results before the training defined as baseline including both groups' subjects. Differences in connectivity of DMN between-groups were tested using a two-sample *t* test and the results were displayed on template anatomic images in neurologic convention. Regions were automatically labeled using the anatomy toolbox atlas *x*, *y*, and *z* MNI coordinates in the left-right anterior-posterior and inferior-superior dimensions, respectively.

#### Results

Demographic characteristics of the subjects are presented in Table 1. As it can be observed, there were no significant differences in age ( $P = 0.118$ ), gender ( $P = 0.453$ ), weight ( $P = 0.860$ ), height ( $P = 0.176$ ), and body mass index ( $P = 0.274$ ) between the groups.

Table 2 shows the effects of IMT on lung and respiratory muscle function. There were no significant changes in FEV<sub>1</sub> ( $P = 0.648$ ), FVC ( $P = 0.480$ ), FEV<sub>1</sub>/FVC ( $P = 0.802$ ), PEF ( $P = 0.101$ ) as pulmonary function testing variables, MEP ( $P = 0.110$ ), and respiratory muscle endurance time ( $P = 0.705$ ) between IMT and sham groups after the training. The MIP, S-index and PIF were significantly improved in the IMT group compared to the sham group at the end of 8th week. Table 3 shows the results obtained from SLP before and after the training. No statistically significant differences were observed in respiratory rate ( $P = 0.344$ ),  $T_i$  ( $P = 0.222$ ),

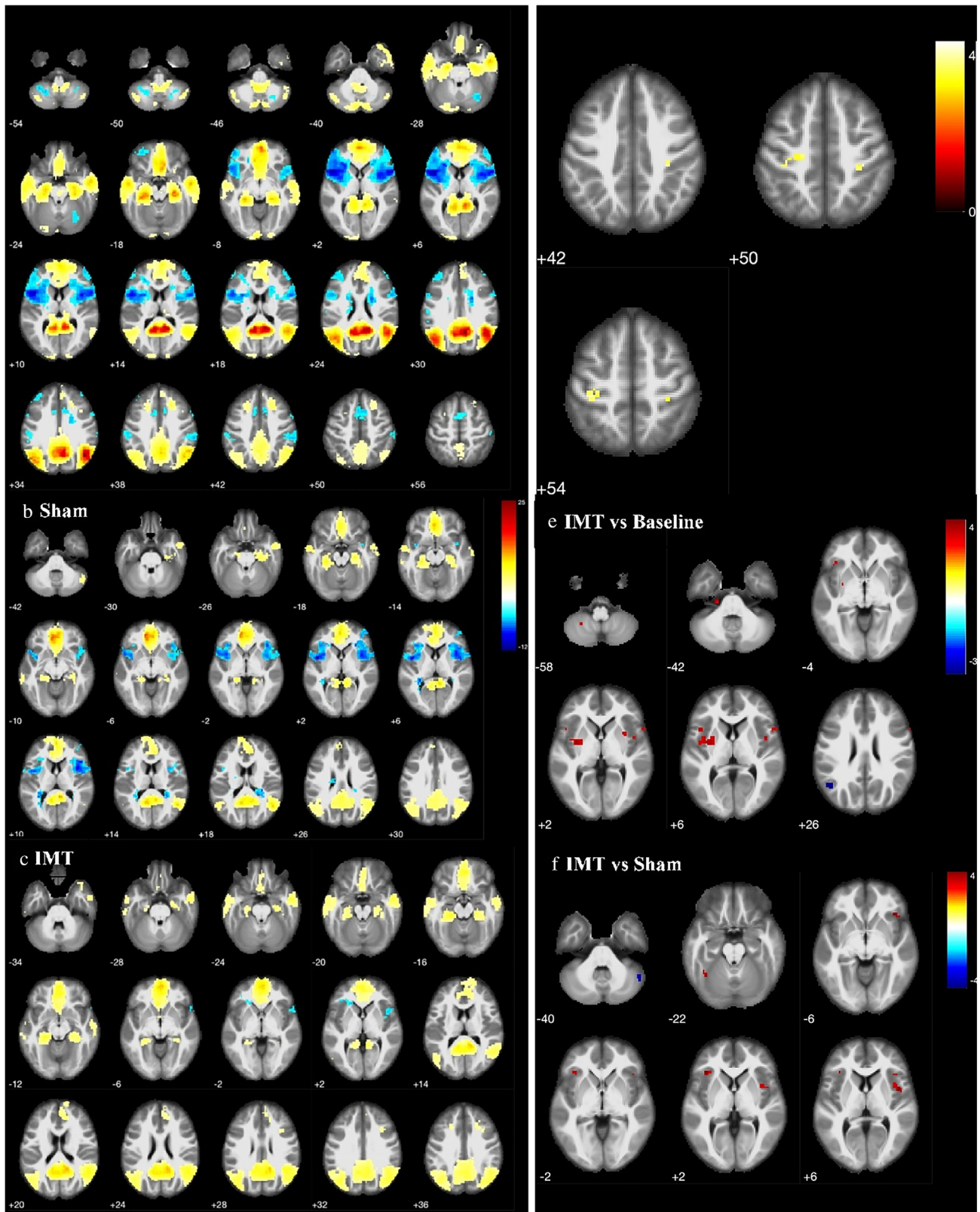


**FIGURE 2:** DMN activation maps are shown (in neurologic convention) in groups separately before (a), and after IMT (b, sham; c, IMT). After 8 weeks of IMT, insula deactivations with DMN regions show significant reduction ( $P < 0.001$ ). Comparison of groups increased activation in bilateral postcentral gyrus in sham group than baseline (d). Comparison of IMT and baseline, IMT group reveals greater activation in the bilateral insula, left putamen, bilateral inferior frontal gyrus, and left cerebellum in the IMT group than baseline and deactivation in the left middle temporal gyrus (e). Greater activation in bilateral inferior frontal gyrus, right insula, left cerebellum and decreased activation right cerebellum in IMT group than sham (f).

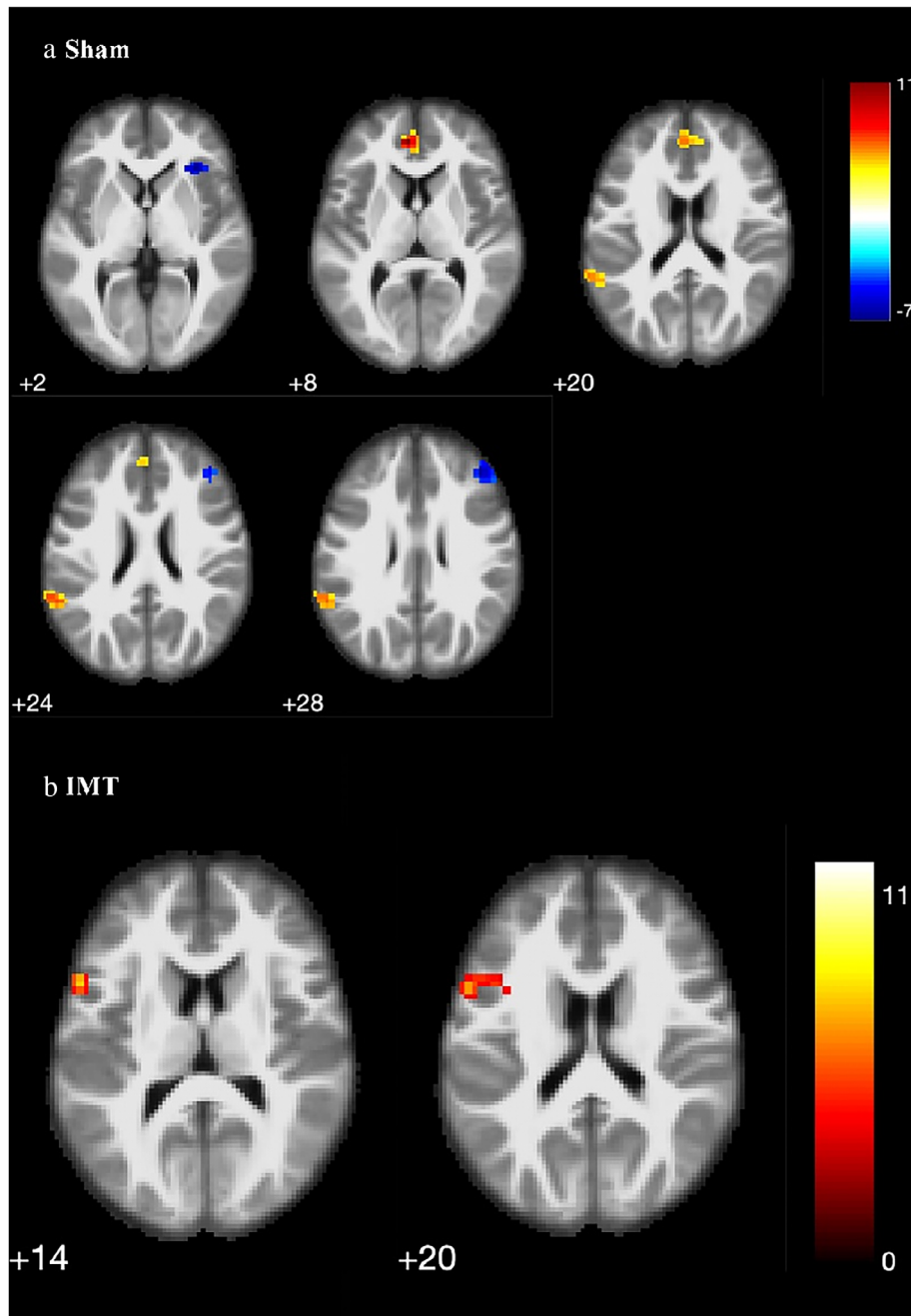


**FIGURE 3:** Activation maps showing the regions (in neurologic convention) having positive (red) and negative (blue) correlations with MEP test within DMN in the sham group. Left ACC, right ACC, left Superior temporal gyrus show positive correlation (from red to orange color). Right middle frontal gyrus, right insula, show negative correlation (blue color) (a). Left IFG (pars triangularis) and left IFG (pars opercularis) show positive correlations with  $T_i/T_{tot}$  test within DMN in the IMT (b).

$T_E$  ( $P = 1.000$ ),  $T_i/T_E$  ( $P = 0.609$ ),  $T_{tot}$  ( $P = 0.501$ ),  $T_i/T_{tot}$  ( $P = 0.572$ ), relative contribution of abdomen to each breath ( $P = 0.851$ ), and IE50 ( $P = 1.000$ ) of thoracic mobility parameters after IMT.

### Imaging

**DEFAULT MODE NETWORK.** Table 4 presents the anatomical regions along with  $x$ ,  $y$ ,  $z$  coordinates, cluster size and

strength of the significant clusters at  $P < 0.05$  ( $p$ -FDR corrected) for DMN.

Default mode network pattern was similar in groups (Fig. 2a–c). However, there were alterations in DMN in terms of activation strengths and cluster sizes following training, more prominent in the IMT group (Table 4). Significant cluster sizes and activation strengths at each defined component of the DMN showed reduction in both sham and intervention groups, more prominently in the IMT group.

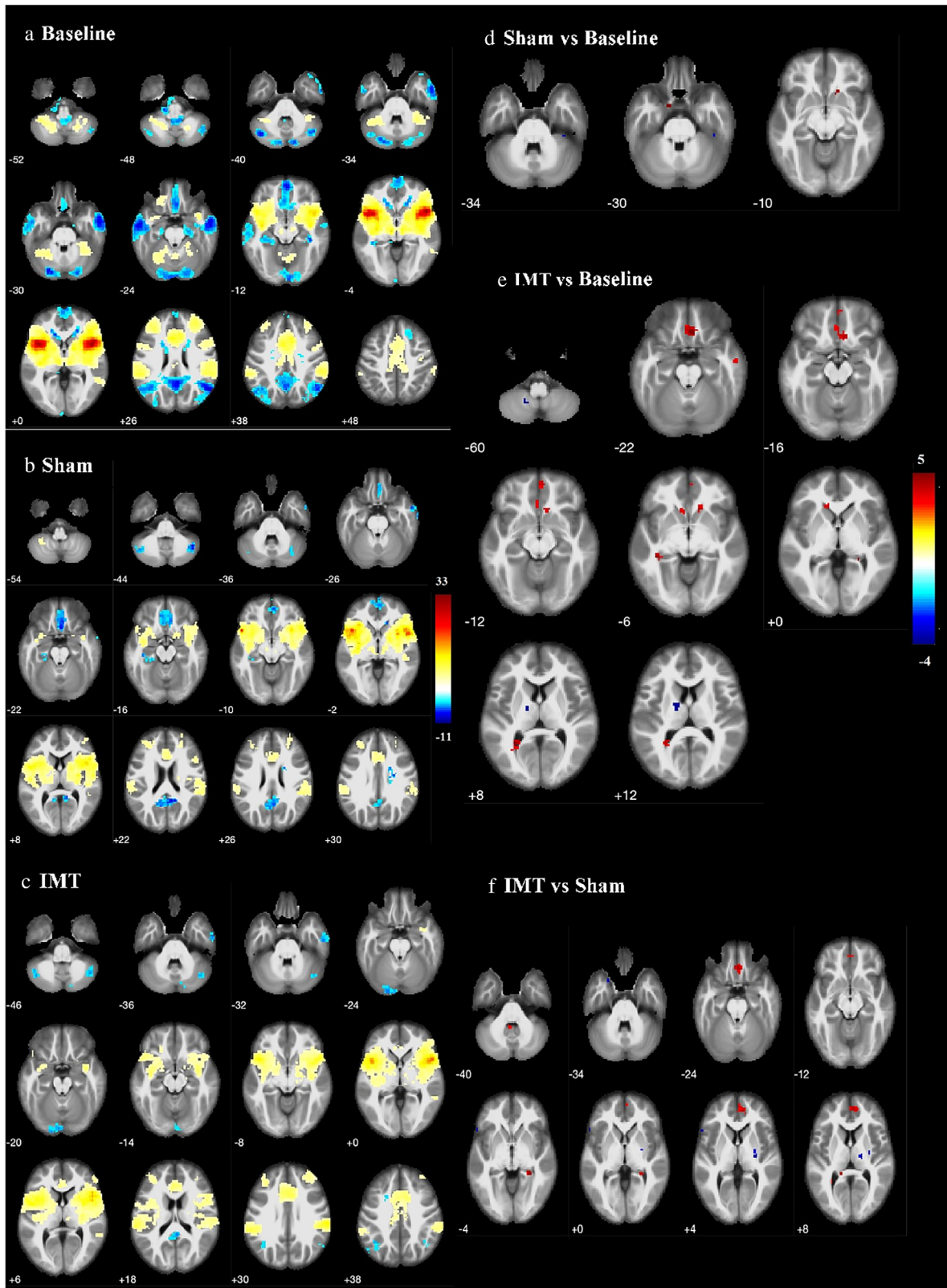


**FIGURE 4:** Bilateral insula network and connectivity maps are shown (in neurologic convention) in the groups separately before (a), and after IMT (b, sham; c, IMT). Insula activation shows reduction and ACC shows increased strength and extent of activation in the IMT group after training (c) compared to baseline map (a) ( $P < 0.001$ ). Comparison of groups increased activation in rectal gyrus and decreased activation in right cerebellum in sham than baseline (d). IMT group reveals greater activation in right rectal gyrus, right parahippocampal gyrus, right IFG and decreased activation in left cerebellum than baseline (e). It shows greater activation of left cerebellum, right superior medial gyrus, rectal gyrus, right parahippocampal gyrus, right middle orbital gyrus, left hippocampus, and greater deactivation of right thalamus, right pallidum, right IFG and left middle temporal pole in IMT group than sham (f).

**TABLE 5. Significant Clusters ( $P < 0.05$  FDR Corrected) Within Bilateral Insula Network in the Groups Are Shown in Terms of Cluster Size and Strengths of Activation and Deactivations With MNI  $x,y,z$  Coordinates**

Groups	Regions	Cluster	$t$ value	$x$	$y$	$z$
	Positive					
	Right insula	34,471	26.9	44	12	-4
	Left insula	33,471	28.2	-38	12	-4
Baseline variables	ACC	4931	11.7	-6	14	32
	Negative					
	MPFC	4294	-8.2	0	54	-12
	Right LP	7592	-8.9	54	-64	26
	Left LP	7592	-8.0	-42	-64	30
	PCC	7592	-8.4	0	-54	32
	Positive					
	Right insula	16,760	25.0	50	8	0
	Left insula	16,760	13.1	-30	10	-6
Sham group	MPFC	1144	6.9	4	20	-22
	Right LP	-	-	-	-	-
	Left LP	-	-	-	-	-
	ACC	1005	7.2	0	18	30
	Negative					
	PCC	990	-8.3	6	-44	14
	Positive					
	Right insula	9512	19.8	48	12	0
	Left insula	8884	12.8	-42	8	-6
	MPFC	-	-	-	-	-
IMT group	Right LP	-	-	-	-	-
	Left LP	-	-	-	-	-
	ACC	2877	9.1	10	12	36
	Negative					
	PCC	156	-5.6	4	-46	18
	Positive					
	Right rectal gyrus	10	3.47	12	18	-10
Sham vs. baseline	Negative					
	Right cerebellum	12	-4.09	38	-34	-34
	Positive					
	Right rectal gyrus	296	4.62	12	24	-6

TABLE 5. Continued

Groups	Regions	Cluster	<i>t</i> value	<i>x</i>	<i>y</i>	<i>z</i>
IMT vs. baseline	Right parahippocampal gyrus	22	4.26	24	-40	0
	Right IFG	16	3.56	58	-10	-22
	Negative					
	Left cerebellum	13	-3.79	-18	-60	-60
	Positive					
	Right superior medial gyrus	137	5.02	6	50	6
	Medial frontal cortex	163	4.84	0	30	-24
IMT vs. sham	Right parahippocampal gyrus	28	4.76	28	-40	-4
	Left hippocampus	12	4.24	-14	-40	8
	Left cerebellum	16	3.93	-6	-52	-40
	Right rectal gyrus	13	3.57	4	48	-12
	Right middle orbital gyrus	137	3.46	4	50	4
	Negative					
	Right thalamus	47	-4.57	16	-12	6
	Right pallidum	51	-4.31	28	-16	2
	Right IFG	54	-3.87	52	18	20
	Left medial temporal pole	16	-3.64	-26	14	-34

Positive: Activated brain regions to the insula network. Negative: Deactivated brain regions to the insula network.  
 ACC = anterior cingulate cortex; MPFC = medial prefrontal cortex; LP = lateral parietal; PCC = posterior cingulate cortex;  
 IMT = inspiratory muscle training.

Deactivation of bilateral insula with DMN also showed significant reduction in both groups, profoundly in the IMT group compared to baseline. Group comparisons of DMN following IMT revealed greater activations in bilateral post-central gyrus in sham compared to baseline results (Fig. 2d). Bilateral insula, left putamen, bilateral inferior frontal gyrus (IFG), and left cerebellum showed increased activation in IMT group compared to baseline results (Fig. 2e). Right insula, bilateral IFG, and left cerebellum, showed increased activation while the right cerebellum showed lesser deactivation in the IMT group than sham (Fig. 2f).

In addition, there were common regions which showed positive and negative correlations with MEP test in sham group (Fig. 3a). Those regions include right and left ACC, left superior temporal gyrus for positive correlations and right middle frontal gyrus, right insula for negative correlations within DMN (Fig. 3a). But there was no correlation between brain regions with MIP, Sindex, IE50,  $T_i/T_{tot}$  tests within DMN. In IMT group left IFG (pars triangularis) and left IFG (pars opercularis) showed positive correlations with  $T_i/T_{tot}$  test within DMN (Fig. 3b).

**INSULA (BILATERAL) NETWORK.** Insula activation and connectivity with the other brain regions differed across the groups. Significant clusters at  $P < 0.05$  FDR corrected were shown in Fig. 4a–c, Table 5. Expectantly, there were deactivation areas including PCC, LP, MPFC within the insula network, which are DMN components. Although to a lesser extent, significant diminished deactivation occurred in these regions (Table 5) after treatment especially in the IMT group. The PCC deactivations showed the most remarkable reduction in the IMT group.

Insula activation was reduced and ACC activation was increased in terms of both activation strength and cluster size in the IMT group after the training (Fig. 4c). Group comparison of the insula following IMT revealed greater activations in rectal gyrus and decreased activation in right cerebellum in sham than baseline results (Fig. 4d). The IMT group revealed greater activation in right rectal gyrus, right parahippocampal gyrus, right IFG and decreased activation in left cerebellum than baseline (Fig. 4e). The IMT group revealed greater activation in the left cerebellum, right superior medial gyrus, rectal gyrus, right parahippocampal gyrus, right middle orbital

gyrus, left hippocampus and greater deactivation in the right thalamus, right pallidum, right IFG than the sham group (Fig. 4f, Table 5).

Within the insula network, there were no correlating brain regions with MIP, MEP, S-index, IE50,  $T_i/T_{tot}$  tests.

## Discussion

The results of this study showed that IMT enhanced respiratory muscle strength and caused significant brain changes in the DMN and insula networks assessed by RS-fMRI in healthy subjects. Following the intervention, all DMN components showed decreased activation, but the insula, which has an anticorrelation with the DMN, showed increased activation. After IMT, however, there was no change in respiratory patterns as measured by SLP. Respiratory muscle strength was positively correlated with activity changes in the brain's stimulus network (ACC, left superior temporal gyrus) but were negatively correlated with activity in the right middle frontal gyrus, right insula. Breathing patterns were positively correlated with left IFG. There have been neuroimaging studies investigating brain activity in different breathing patterns (slow breathing, quick breathing, breath holding, single breath loading, and so on),<sup>22–25</sup> but this study investigates brain activity in long-term respiratory muscle training. Raux et al.<sup>22</sup> discovered that persistent inspiratory stress in a single session can aid motor reorganization by reducing phrenic motoneuron recruitment. This adaptive technique may improve the efficiency of the respiratory muscles during inspiration by optimizing respiratory muscle recruitment during persistent inspiratory loads. Sustained inspiratory muscle loading was shown to diminish cortical activation in premotor, motor, and sensory cortical areas in one investigation using fMRI<sup>23</sup>. These findings imply that after inspiratory loading, the central respiratory drive undergoes significant reconfiguration, which could explain some of the changes in respiratory muscle efficiency.<sup>26</sup> How S et al.<sup>27</sup> assessed acute and chronic effects of IMT on upper airways using a MRI in healthy subjects. They found changes in upper airway morphology and narrowing after IMT. However, we evaluated the responses of IMT on brain activity using a fMRI.

In this work, the insula network showed greater activation after the IMT intervention. This result corroborates the fact that the insula is a region of a brain network that processes interoceptive information and hedonic appraisal and combines sensory inputs with conscious and unconscious processes like decision-making, emotions, pain, memory, motivation, and arousal.<sup>26</sup> Additionally, anticipatory changes in brain activity in other areas for emotion processing, such as the cingulate cortex, prefrontal cortex, amygdala, cerebellum, and midbrain/periaqueductal gray matter, have been identified<sup>28</sup> and investigated in various neuroimaging studies of breathlessness perception.<sup>29,30</sup> The sensation of being out of breath stimulates the upper airway and other respiratory muscles, which can provide a huge source of motivation for

inspiring initiatives.<sup>31</sup> This suggests that increasing respiratory muscle strength aided healthy people in this study in improving the accuracy of their breathing predictions for a forthcoming stimulus. These expectations are matched with sensory input from the peripheral, allowing the brain to generate the appropriate perception. Attention and interoceptive ability are also thought to influence this system by altering prior expectations and experiences or incoming sensory information.<sup>3,32</sup> In addition, inspiratory muscle exercise increases hippocampal gyrus responsiveness. Although the role of the hippocampi in breathing perception is unknown, stimulation affected breathing patterns and revealed linkages between neuronal discharge and breathing patterns. The findings point to the hippocampus acting as an auxiliary or compensation mechanism to help the brain cope with the protracted challenge.<sup>33</sup> Therefore, IMT may develop breathlessness expectations and pay more attention to breathing perception, as well as improve the processing of respiratory signals for more accurate ventilator interoception in healthy individuals.

In this study, the deactivated regions were found in the MPFC, LP, and PCC after IMT. Activation of the insula reduces DMN activation.<sup>34,35</sup> The DMN competes with the majority of task-related networks, and suppression of the DMN is frequently associated with the activation of a cognitive task-related network.<sup>23</sup> In task-fMRI investigations, it has been shown that connection within DMN areas helps to facilitate or monitor cognitive performance, and changes in functional coupling within DMN regions can predict differences in cognitive performance.<sup>36</sup> The DMN deactivates during cognitive tasks, with a magnitude that varies depending on the task's difficulty.<sup>23</sup> DMN deactivation following IMT in our subjects may have occurred because of their improved attention to the task. Furthermore, DMN deactivation could be linked to the interoceptive processing of dyspnea sensations.<sup>37</sup> Breathing muscle performance may be affected by changes in breathlessness perception. Deactivation of corollary discharge between the motor and sensory cortices can help to improve respiratory muscle strength.<sup>26</sup>

The correlation between respiratory muscle strength and changes in brain activity seen in the right and left ACC, left superior temporal gyrus with DMN after IMT suggests that reappraisal of learned associations may also influence lower-order sensory processing. With parasympathetic outflow, the left insula has a large influence on autonomic regulation.<sup>38</sup> The activation of the left-side anterior insula, a region associated with interoception, or the conscious awareness of physiological sensations, was linked to breathlessness scores.<sup>39</sup> In the right middle frontal gyrus, right insula, left superior temporal gyrus of fMRI activity was negatively linked with respiratory muscle strength. The inverse connection between brain activity and respiratory parameters suggests a significant difference in prior, anticipatory brain activity directed toward subjective perceptions following IMT administration.<sup>24</sup> These alterations in brain activity could

indicate a shift in expectation in the direction of healthy controls.<sup>40</sup> It is possible that the IMT's 8-week loading helped reshape connections. This changed connectivity between the interoceptive attention network and the primary sensorimotor cortex aids in the processing of incoming and outgoing respiratory information, which could be linked to more accurate ventilatory perceptions.

SLP measurements revealed no significant differences in breathing patterns or regional respiratory functioning between the two groups. The impact of IMT on breathing patterns measured using SLP is feasible and easy to implement in healthy individuals. Healthy people have normal tidal breathing characteristics, and we have observed no change following the training. Ideal efficiency of SLP in patients with thoracoabdominal synchronization caused by greater work of breathing requires further investigation.

### Limitations

A potential limitation of the present study is not assessing cognitive effects of IMT intervention. However, our primary purpose was to understand brain networks of group effects of IMT compared with sham-treated subjects. Furthermore, our findings, which were based on young healthy subjects not in large numbers, cannot be applied to patients with lung diseases, particularly those with chronic dyspnea. We could have done a thorax MRI instead of a spirometry assessment to see the improvement in lung ventilation. However, we use SLP as a novel technique for thoracic activity. More research is needed to better understand brain activity in patients with chronic respiratory disease after IMT intervention.

### Conclusion

IMT showed positive achievements as a training method on physiologic brain mechanisms in healthy subjects. IMT improved respiratory muscle strength and caused significant brain activity and connectivity changes in the default mode network and insula networks assessed by RS-fMRI. These changes may improve in ventilatory perception and may regulate breathing pattern by processing interoceptive signals with high-intensity IMT. It may have an important role in adaptation in respiratory health.

### Acknowledgments

The study was cofounded by Hacettepe University Scientific Research Unit (THD-2020-18816). The authors thank the participating individuals, as well as the National Magnetic Resonance Research Center (UMRAM) staff.

### Conflict of interests

The authors have no financial or ethical conflicts of interest regarding the contents of this manuscript.

### Ethics approval

All participants included in the study signed the informed consent and the research was approved by the university's ethics committee and Ministry of Health.

### References

1. Finnegan SL, Harrison OK, Harmer CJ, et al. Breathlessness in COPD: Linking symptom clusters with brain activity. *Eur Respir J* 2021;58:2004099.
2. Herigstad M, Faull OK, Hayen A, et al. Treating breathlessness via the brain: Changes in brain activity over a course of pulmonary rehabilitation. *Eur Respir J* 2017;50:1701029.
3. Faull OK, Hayen A, Pattinson KTS. Breathlessness and the body: Neuroimaging clues for the inferential leap. *Cortex* 2017;95:211-221.
4. Logothetis NK, Pauls J, Augath M, Trinath T, Oeltermann A. Neurophysiological investigation of the basis of the fMRI signal. *Nature* 2001;412:150-157.
5. Raichle ME, MacLeod AM, Snyder AZ, Powers WJ, Gusnard DA, Shulman GL. A default mode of brain function. *Proc Natl Acad Sci U S A* 2001;98:676-682.
6. Huang CH, Martin AD, Davenport PW. Effect of inspiratory muscle strength training on inspiratory motor drive and RREP early peak components. *J Appl Physiol* 2003;94:462-468.
7. Witt JD, Guenette JA, Rupert JL, McKenzie DC, Sheel AW. Inspiratory muscle training attenuates the human respiratory muscle metaboreflex. *J Physiol* 2007;584:1019-1028.
8. Sheel AW. Respiratory muscle training in healthy individuals: Physiological rationale and implications for exercise performance. *Sports Med* 2002;32:567-581.
9. Ramsok AH, Molgat-Seon Y, Schaeffer MR, et al. Effects of inspiratory muscle training on respiratory muscle electromyography and dyspnea during exercise in healthy men. *J Appl Physiol* 2017;122:1267-1275.
10. Sasaki M, Kurosawa H, Kohzaki M. Effects of inspiratory and expiratory muscle training in normal subjects. *J Jpn Phys Ther Assoc* 2005;8:29-37.
11. Hart N, Sylvester K, Ward S, Cramer D, Moxham J, Polkey MI. Evaluation of an inspiratory muscle trainer in healthy humans. *Respir Med* 2001;95:526-531.
12. Figueiredo RIN, Azambuja AM, Cureau FV, Sbruzzi G. Inspiratory muscle training in COPD. *Respir Care* 2020;65:1189-1201.
13. Herigstad M, Hayen A, Wiech K, Pattinson KT. Dyspnoea and the brain. *Respir Med* 2011;105:809-817.
14. Charususin N, Gosselink R, McConnell A, et al. Inspiratory muscle training improves breathing pattern during exercise in COPD patients. *Eur Respir J* 2016;47:1261-1264.
15. Simon N, Hussain A, Kolvekar P, Kolvekar S. Feasibility of structured light plethysmography (SLP) in patients with coronavirus disease 2019 (COVID-19). *J Cardiothorac Surg* 2021;16:20.
16. Miller MR, Crapo R, Hankinson J, et al. General considerations for lung function testing. *Eur Respir J* 2005;26:153-161.
17. Laveneziana P, Albuquerque A, Aliverti A, et al. ERS statement on respiratory muscle testing at rest and during exercise. *Eur Respir J* 2019;53:1801214.
18. Silva PE, de Carvalho KL, Frazão M, Maldaner V, Daniel CR, Gomes-Neto M. Assessment of maximum dynamic inspiratory pressure. *Respir Care* 2018;63:1231-1238.
19. Elshafie G, Kumar P, Motamedi-Fakhr S, Iles R, Wilson RC, Naidu B. Measuring changes in chest wall motion after lung resection using structured light plethysmography: A feasibility study. *Interact Cardiovasc Thorac Surg* 2016;23:544-547.

20. Motamedi-Fakhr S, Iles R, Barker N, Alexander J, Cooper BG. Reference equations for tidal breathing parameters using structured light plethysmography. *ERJ Open Res* 2021;7:00050-02021.
21. Whitfield-Gabrieli S, Nieto-Castanon A. Conn: A functional connectivity toolbox for correlated and anticorrelated brain networks. *Brain Connect* 2012;2:125-141.
22. Raux M, Demoule A, Redolfi S, Morelot-Panzini C, Similowski T. Reduced phrenic motoneuron recruitment during sustained inspiratory threshold loading compared to single-breath loading: A twitch interpolation study. *Front Physiol* 2016;7:537.
23. Raux M, Tyvaert L, Ferreira M, et al. Functional magnetic resonance imaging suggests automatization of the cortical response to inspiratory threshold loading in humans. *Respir Physiol Neurobiol* 2013;189:571-580.
24. Faull OK, Cox PJ, Pattinson KTS. Cortical processing of breathing perceptions in the athletic brain. *Neuroimage* 2018;179:92-101.
25. Tremoureux L, Raux M, Jutand L, Similowski T. Sustained preinspiratory cortical potentials during prolonged inspiratory threshold loading in humans. *J Appl Physiol* 2010;108:1127-1133.
26. Shei RJ. Recent advancements in our understanding of the ergogenic effect of respiratory muscle training in healthy humans: A systematic review. *J Strength Cond Res* 2018;32:2665-2676.
27. How SC, McConnell AK, Taylor BJ, Romer LM. Acute and chronic responses of the upper airway to inspiratory loading in healthy awake humans: An MRI study. *Respir Physiol Neurobiol* 2007;157:270-280.
28. Haase L, May AC, Falahpour M, et al. A pilot study investigating changes in neural processing after mindfulness training in elite athletes. *Front Behav Neurosci* 2015;9:229.
29. Stoeckel MC, Esser RW, Gamer M, Büchel C, von Leupoldt A. Brain responses during the anticipation of dyspnea. *Neural Plast* 2016;2016:6434987.
30. Peiffer C, Poline JB, Thivard L, Aubier M, Samson Y. Neural substrates for the perception of acutely induced dyspnea. *Am J Respir Crit Care Med* 2001;163:951-957.
31. da Fonsêca JDM, Resqueti VR, Benício K, Fregonezi G, Aliverti A. Acute effects of inspiratory loads and interfaces on breathing pattern and activity of respiratory muscles in healthy subjects. *Front Physiol* 2019;10:993.
32. Phelps EA, Ling S, Carrasco M. Emotion facilitates perception and potentiates the perceptual benefits of attention. *Psychol Sci* 2006;17:292-299.
33. Macey PM, Macey KE, Henderson LA, et al. Functional magnetic resonance imaging responses to expiratory loading in obstructive sleep apnea. *Respir Physiol Neurobiol* 2003;138:275-290.
34. Zhang S, Wu W, Huang G, et al. Resting-state connectivity in default mode network and insula during experimental low back pain. *Neural Regen Res* 2014;9:135-142.
35. Hölzel BK, Ott U, Hempel H, et al. Differential engagement of anterior cingulate and adjacent medial frontal cortex in adept meditators and non-meditators. *Neurosci Lett* 2007;421:16-21.
36. Sala-Llonch R, Peña-Gómez C, Arenaza-Urquijo EM, et al. Brain connectivity during resting state and subsequent working memory task predicts behavioural performance. *Cortex* 2012;48:1187-1196.
37. van Oudenhove L, Vandenberghe J, Dupont P, et al. Cortical deactivations during gastric fundus distension in health: Visceral pain-specific response or attenuation of 'default mode' brain function? A H2 15O-PET study. *Neurogastroenterol Motil* 2009;21:259-271.
38. Shoemaker JK, Goswami R. Forebrain neurocircuitry associated with human reflex cardiovascular control. *Front Physiol* 2015;6:240.
39. Allard E, Canzoneri E, Adler D, et al. Interferences between breathing, experimental dyspnoea and bodily self-consciousness. *Sci Rep* 2017;7:9990.
40. Herigstad M, Hayen A, Evans E, et al. Dyspnea-related cues engage the prefrontal cortex: Evidence from functional brain imaging in COPD. *Chest* 2015;148:953-961.